Computational investigations of eighteen-electron triatomic sulfur-nitrogen anions

Juuso Valjus, Heikki M. Tuononen, Risto S. Laitinen, and Tristram Chivers

J. Valjus and H. M. Tuononen, Department of Chemistry, Nanoscience Centre, P.O. Box 35, FI-40014 University of Jyväskylä, Finland

R. S. Laitinen,† Laboratory of Inorganic Chemistry, Environmental and Chemical Engineering, P.O. Box 3000, FI-90014 University of Oulu, Finland

T. Chivers,† Department of Chemistry, University of Calgary, 2500 University Drive NW, Calgary, Alberta, T2N 1N4, Canada

†**Corresponding authors**: [e-mail: chivers@ucalgary.ca, tel. +1(403)2205741; risto.laitinen@oulu.fi, tel. +358(294)481611]

Keywords*:* sulfur-nitrogen anions, eighteen-electron triatomics, isomers, electronic structures, theoretical calculations

Abstract:

MRCI-SD/def2-QZVP and PBE0/def2-QZVP calculations have been employed for the analysis of geometries, stabilities, and bonding of different isomers of the eighteen-electron anions N_2S^{2-}, NS_2^-, and NSO^-. Isomers of the isoelectronic neutral molecules SO_2, S_2O, S_3, and O_3 have been included for comparison. The sulfur-centered acyclic NSN^{2-} (**1a**), NSS^- (**2b**), and NSO^- (**3a**) anions are the most stable isomers of their respective molecular compositions. However, the nitrogen-centered isomers SNS^- (**2a**) and SNO^- (**3b**$_2$) lie close enough in energy to their more stable counterparts to allow their occurrence. The experimental structural information, where available, is in good agreement with the optimized bond parameters. The optimized geometries of OSO (**4a**), OSS (**5b**), and OOO (**7a**) also agree with experimental data. The bonding in all investigated species is qualitatively similar, though electron density analyses reveal important quantitative differences that arise from bond polarization. Most of the investigated systems can be described with a single configuration wave function, the two notable exceptions being isomers SSS (**6a**) and OOO (**7a**) that show some diradical character.

The computed MRCI-SD/def2-QZVP absorption maxima for SNS^- (**2a**) and NSS^- (**2b**) are 342 and 327 nm, respectively. The corresponding PBE0/def2-QZVP values in acetonitrile are 353 and 333 nm. These data support the formation of SNS^- in electrochemical or chemical reduction of $SSNS^-$, which has been proposed on the basis of UV-visible absorption bands at λ_{max} 375 nm in acetonitrile or 390 nm in liquid NH_3. Although SNS^- is less stable than NSS^-, their interconversion is calculated to be facile and reversible, leading to an equilibrium solution from which SNS^- can be detected by its absorption. Thus, salts of the binary sulfur-nitrogen anion S_2N^-, as either **2a** or

2b, with bulky organic cations or crown-ether solvated alkali-metal cations represent feasible synthetic targets.

Introduction

Binary S,N and ternary N,S,O anions have engendered interest recently owing to their involvement in processes ranging from biological signaling to atmospheric chemistry.[1] The eighteen-electron triatomic anions NSO^- and NSN^{2-}, isoelectronic with SO_2, were first prepared and isolated as potassium salts in 1979 and 1982, respectively.[2,3] The soluble tris(dimethylamino)sulfonium salt $[(Me_2N)_3S](NSO)$ has also been isolated.[4] Although the structures of M(NSO) (M = K, Rb) have been determined by X-ray powder diffraction analysis[5] and single crystals of $(Me_4N)(NSO)$ have also been obtained,[6] the reported structural parameters are unreliable because O and N atoms could not be distinguished due to crystallographic disorder in the lattice. In contrast, an accurate structural determination of the $[K(18\text{-crown-}6)]^+$ salt of NSN^{2-} has been reported;[7] the dianion exhibits slightly longer S-N bond lengths compared to the corresponding S-O distances in the neutral SO_2 molecule (S-N, 1.484(3) Å vs. S-O, 1.4297(4) Å) and the ESE bond angle is significantly widened (NSN, 129.9(2)° vs. OSO, 117.5(1)°). The bent NSO^- (C_s) and NSN^{2-} (C_{2v}) anions give rise to simple IR spectra comprised of asymmetric and symmetric stretching modes (ν_{as} and ν_s) and a bending mode (δ). The stretching modes for NSN^{2-} occur at lower frequencies (by 150-160 cm^{-1}) than those for SO_2.[1] The similar values of all three vibrations for NSO^- salts indicate only minor anion-cation interactions in the solid state.[5] Consistently, a recent photoelectron spectroscopy study of NSO^- provided values for the fundamental vibrations in good agreement with the IR data.[8]

Although the NSO^- and NSN^{2-} anions have been employed in metathetical reactions to generate main group element and transition-metal complexes,[1,9] there have been relatively few computational studies of these fundamentally important species. An early investigation of the NSN^{2-} dianion by a combination of Hartree-Fock-Slater (HFS) and semi-empirical MNDO methods predicted two vastly different geometries,[10] whereas more recent computational work using 2nd order Møller-Plesset perturbation theory (MP2) and density functional theory (DFT) has reproduced the experimental geometry;[7] the bonding in the cyclic isomer of NSN^{2-} has been discussed at the semi-empirical CNDO/2 level of theory.[11]

The relative stability of the structural isomers NSO^- and SNO^- has been of topical interest owing to the biological significance of the latter species.[12] While the first computational investigations employed mostly non-correlated levels of theory,[13,14,15] recent studies have used highly correlated *ab initio* methods to confirm that NSO^- is substantially more stable than SNO^-, with an energy barrier greater than 450 kJ mol^{-1} for intramolecular isomerization.[16] A DFT-level bonding analysis of NSO^- revealed the expected four-electron three-centre π-system with a high S-N bond order and significantly weaker S-O interaction.[17] Contemporary investigations of the electronic structure of the isoelectronic SO_2 molecule have focused on the correlation between diradical character and molecular properties[18] as well as its reaction with hydrogen atoms.[19]

The related eighteen-electron triatomic anion NS_2^- is also of considerable interest and has to date eluded isolation.[1] However, its formation from the electrochemical or chemical (with NH_2^-) reduction of $SSNS^-$ has been proposed on the basis of the observation of absorption maxima (λ_{max}) at 375 nm in acetonitrile or 390 nm in liquid NH_3, respectively (see Scheme 1).[20,21] The reduction process involves S-S bond cleavage, which is expected to occur upon addition of an electron to the lowest unoccupied molecular orbital (LUMO) of $SSNS^-$ that is strongly antibonding with

respect to the S-S linkage.[22] Although mass spectrometric techniques support S-S-N-S connectivity for neutral and ionic NS_3 species in the gas phase, this methodology was not able to distinguish between an acyclic N-S-S arrangement and a cyclic structure for the related NS_2 species.[23] The previous computational studies of NS_2^- were reported close to 30 years ago.[24,25] While the first study employed the HFS method, the latter used the significantly more accurate multireference configuration interaction MRCI-D approach, allowing the estimation of both structural and spectroscopic parameters of NS_2^- at a very high level of theory.

(Scheme 1 here)

In this contribution, we explore the geometries, relative stabilities and some spectroscopic properties of the different possible isomers of the eighteen-electron triatomic anions N_2S^{2-}, NSO^-, and NS_2^-.[a] While there are numerous computational and experimental studies involving the isoelectronic species SO_2, S_2O, O_3, and S_3,[18,26] these molecules have nevertheless been included in the current study for comparison purposes. All single configuration computations were carried out at the PBE0/def2-QZVP level, while multireference calculations were performed at the MRCI-SD/def2-QZVP level.

[a] The generic formulae N_2S^{2-}, NS^{2-}, NSO^-, SO_2, S_2O, S_3 are used, when only composition is being specified. When considering actual isomers, the order of the atomic symbols indicate connectivity (*i.e.* NSN^{2-} for **1a**).

Computational details

The molecules and anions considered in this contribution are shown in Fig. 1. An initial structure search for each molecule and anion was performed with Gaussian09,[27] employing the PBE0 hybrid density functional[28,29,30,31] and Ahlrichs'quadruple-ζ valence def2-QZVP basis sets.[32] The bond angles were varied in steps of 10° from 30° to 180°, setting the electronic state of the molecules and anions either to a singlet, a triplet, or a broken-symmetry singlet. This search yielded local minima for wide-angle acyclic isomers as well as for small-angle cyclic isomers. The results were subsequently checked for internal instabilities and, if needed, re-optimized within the broken-symmetry framework.

(Fig. 1 here)

The PBE0/def2-QZVP optimized geometry corresponding to the lowest Gibbs energy for each unique acyclic and cyclic isomer was used as a starting point for calculations with more accurate wave function methods using MOLPRO 2015.1.[33,34] First, full valence complete active space CASSCF/def2-QZVP [35,36] calculations were executed to generate starting orbitals for successive multireference configuration interaction MRCI-SD/def2-QZVP calculations and geometry optimizations.[37] These calculations were performed in order to treat molecules and anions with variable amounts of diradical character on equal footing. Vibrational frequency analyses using the numerical MRCI-SD Hessian method were performed to confirm the nature of all stationary points found (minimum or transition state). The MRCI-SD natural orbitals corresponding to the optimized structures were subsequently utilized to calculate generalized Wiberg bond orders

(gWBOs)[38] and Atoms in Molecules (AIM) delocalization indices (DIs)[39] with programs Molden2AIM[40] and AIMAll.[41] Images of MRCI-SD natural orbitals were drawn with the program Jmol.[42]

The absorption properties of SNS^- and NSS^- were calculated at both MRCI-SD and PBE1PBE levels of theory, the latter employing the time-dependent (TD-DFT) approach.[43] In DFT calculations, the integral equation formalism variant of the polarizable continuum model (IEFPCM) was used to model the effect of the solvent (acetonitrile) on the absorption properties of SNS^- and NSS^- as well as on their interconversion (reaction energies).[44]

Results and discussion

Geometries and energetics

The MRCI-SD/def2-QZVP optimized geometries and relative energies of all isomers of each species considered are shown in Table 1; the total energies and the Cartesian coordinates of the atoms are reported in the Supplementary Material (Tables S1 and S2, respectively).

(Table 1 here)

Isomers of N_2S^{2-}. There are three possible isomers for the N_2S^{2-} dianion: two acyclic species, NSN^{2-} (**1a**) and NNS^{2-} (**1b**), and the cyclic structure, *c*-NSN^{2-} (**1c**). The symmetric isomer **1a** has been isolated and structurally characterized as $K_2(NSN)^3$ and $[K(18\text{-c-}6)]_2(NSN)$ salts.[7] The MRCI-SD/def2-QZVP optimized bond parameters for **1a** (1.532 Å and 128.3º) agree reasonably

well with the experimental values (see Table 1) and data from earlier calculations employing the MP2 and DFT methods.[7] In contrast, the asymmetric isomer **1b** proved to be an unstable species in vacuum with respect to dissociation to N_2 and S^{2-}, as also found in the early HFS and MNDO calculations.[10] The MRCI-SD/def2-QZVP optimization yielded a local minimum for the cyclic isomer **1c**, but it lies 270 kJ mol^{-1} higher in energy than **1a**. As only a small energy barrier prevents **1c** from dissociating to N_2 and S^{2-}, its preparation cannot be considered likely.

Isomers of NS_2^-. The two acyclic isomers of the NS_2^- anion, SNS^- (**2a**) and NSS^- (**2b**), were found to lie close to each other in energy. Contrary to early HFS work,[24] the MRCI-SD/def2-QZVP calculations indicate that the asymmetric isomer **2b** is more stable than the symmetric isomer **2a**. However, the energy difference is only 25 kJ mol^{-1}, indicating that the occurrence of both isomers is possible; there is no experimental structural information on either of the two species. The MRCI-SD/def2-QZVP computed S-N bond length of 1.649 Å in **2a** is in good agreement with the earlier MRCI-D prediction of 1.66 Å,[25] and much longer than the corresponding bond in NSN^{2-}, 1.532 Å (see Table 1). This suggests a significantly weaker S-N interaction in the former compared to the latter. The lengths of the S-N and S-S bonds in **2b**, 1.496 and 2.036 Å, suggest approximately double and single bonds, respectively. The cyclic isomer *c*-SNS^- (**2c**) exhibits typical single bond lengths with respect to all three bonds, but this isomer lies 177 kJ mol^{-1} above **2b** at the MRCI-SD/def2-QZVP level.

Isomers of NSO^-. There are four isomers with the formula NSO^-. The arrangement NSO^- (**3a**) has the lowest relative energy at the MRCI-SD/def2-QZVP level, but the alternative SNO^- (**3b$_1$**) lies only 89 kJ mol^{-1} above it. In contrast, the third acyclic isomer NOS^- (**3b$_2$**) and the cyclic isomer *c*-NSO^- (**3c**) lie well above **3a** (308 kJ mol^{-1} and 364 kJ mol^{-1}, respectively), and are not discussed further. Experimentally, both **3a** and **3b$_1$** have been isolated and structurally

characterized;[2,4,6,45] their photoelectron spectra have also been reported.[8,16] A comparison between computational and experimental structural data is, however, unwarranted due to crystallographic disorder in the positions of N and O atoms in the structures of **3a** and **3b$_1$**.

Isomers of SO_2. The most stable isomer of SO_2 is, expectedly, the symmetric acyclic OSO (**4a**). The optimized MRCI-SD/def2-QZVP bond parameters of 1.431 Å and 119.5° agree well with the experimental values of 1.4299(4) Å and 117.16(3)° (see Table 1),[46] and with the results from earlier computations at the MRCI-SD/aug-cc-pV(T+d)Z level.[18] While the asymmetric isomer OOS (**4b**) and the cyclic isomer *c*-OSO (**4c**) also show reasonable values for their optimized bond parameters, these isomers lie over 450 kJ mol^{-1} above **4a** at the MRCI-SD/def2-QZVP level and are, therefore, unlikely to be encountered experimentally; an energy difference of 481 kJ mol^{-1} was recently calculated for **4a** and **4b** at the MRCI-SD/aug-cc-pV(T+d)Z level of theory.[18]

Isomers of S_2O.The lowest-energy isomer of S_2O at the MRCI-SD/def2-QZVP level is the asymmetric acyclic OSS (**5b**). The symmetric acyclic arrangement SOS (**5a**) and the cyclic form *c*-SOS (**5c**) lie 254 and 186 kJ mol^{-1} above **5b**, respectively. In good agreement with our calculations, a recent MRCI-SD/aug-cc-pV(T+d)Z study predicted the energy difference of **5b** and **5a** to be 245 kJ mol^{-1}.[18] The isomer OSS (**5b**) can be prepared by treating silver(I) sulfide (Ag_2S) with thionyl chloride ($SOCl_2$).[47,48] The available structural data is based on the determination of a harmonic force field for S_2O from a combined least-squares refinement of fundamental vibrations, isotopic shifts, and centrifugal distortion constants.[49] The reported bond lengths and bond angle are in excellent agreement with the calculated MRCI-SD/def2-QZVP values (see Table 1).

Isomers of O_3 and S_3. The acyclic structure OOO (**7a**) is well-established for O_3 both by experimental[50] and computational methods.[18,26] The existence and stability of the high-energy cyclic isomer *c*-OOO (**7c**), however, have been the subject of extensive interest and debate.[26] Our

computations expectedly reproduce the geometries and relative energies of **7a** and **7c** (see Table 1). In the case of S_3, there is no experimental structural evidence for either the acyclic arrangement SSS (**6a**) or the cyclic isomer *c*-SSS (**6c**). However, all computational studies, including the current one, indicate that while **6a** is the more stable isomer, the cyclic form **6c** lies significantly closer in energy than in the case of O_3 (28 kJ mol^{-1} at the MRCI-SD/def2-QZVP level of theory).[51]

Electronic structures and bonding

The ground states of most of the investigated molecules and anions were either $^1A_1$ or ^1A' at the MRCI-SD/def2-QZVP level of theory (see Table 1). The only exception to the above was the ground state of the high-energy isomer NOS^- (**3b$_2$**) that was found to be ^3A".

Selected MRCI-SD natural orbitals (full valence space) and their occupancies are presented in Fig. 2 for acyclic NSN^{2-} (**1a**), SNS^- (**2a**), NSS^- (**2b**), NSO^- (**3a**), and SNO^- (**3b$_1$**); the corresponding orbitals of OSO (**4a**) are also shown for comparison. It is clear from Fig. 2 that the natural orbitals are qualitatively similar in shape with important variations that mirror the changes in both symmetry and atomic composition of the species in question. For example, the 3*a*''-orbital of NSO^- (**3a**) is of π-type and clearly S-N bonding and S-O anti-bonding, while the matching a_2-symmetric orbitals of OSO, SNS^-, and NSN^{2-} are effectively non-bonding. In similar vein, the corresponding *a*''-symmetric π-type orbitals of NSS^- (**2b**) and SNO^- (**3b$_1$**) are S-N bonding/S-S anti-bonding and N-O bonding/S-N anti-bonding, respectively. These differences naturally arise from the polarization of the electron density in species with inequivalent terminal atoms, and such polarization is by no means limited to π-orbitals but it also affects the σ-framework (see Fig. 2). As a result, the electron density analyses show great variation in the predicted bond properties for **1**-**7** (see below).

(Fig. 2 here)

Fig. 2 also demonstrates that none of the molecules and anions examined herein (N_2S^{2-}, NS_2^-, and NSO^-) has appreciable diradical character as judged by the occupancies of their MRCI-SD natural orbitals. In each case, the highest occupation on formally unoccupied orbitals is not significantly higher than 0.10 e^-. By contrast, the two homonuclear triatomic molecules SSS (**6a**) and OOO (**7a**) show greater multiconfigurational character, with natural orbital occupancies of the unoccupied orbitals of 0.18 and 0.25 e^-, respectively; even higher natural orbital occupancies were obtained for the high-energy isomers OOS (0.32 e^-) and SOS (0.39 e^-). The diradical character in the series of molecules S_xO_{3-x} (x = 0-3) has been the subject of extensive discussion in recent years,[18,52,53,54] with the earlier theoretical calculations yielding the trend OSO ≈ OSS << S_3 < O_3 < OOS < SOS. Our calculations reproduce this result and further show that the isoelectronic replacement of O or S with N^- effectively leads to loss of diradical character in all cases considered. An explanation for this effect has been described before:[55] the level of diradical character in the eighteen-electron triatomics depends on the possibility for charge separation that, in turn, is governed by the electronegativity of the central atom and the size of the two terminal atoms.

The results of bonding analyses for the energetically favourable species **1a**, **2a**, **2b**, **3a**, **3b**$_1$, **4a**, **5b**, **6a**, and **7a** are shown in Table 2. When the optimized bond parameters, gWBOs, and AIM DIs are compared to the generally accepted single and double bond lengths of the S-N, S-O, and S-S bonds (see Table 3),[56,57,58,59] it becomes clear that the gWBOs reproduce rather well the formal bond orders expected on the basis of interatomic distances alone. By contrast, the calculated DIs

show values significantly smaller than the formal bond orders, and especially so in cases when the polarity of the bond (as determined from the AIM atomic charges) is high. This is, however, expected as the gWBO is an index-type measure of the leading non-classical exchange contribution to bonding between two atoms,[38] whereas the DI is not an indicator of bond order but rather a measure of shared electron pairs between two (AIM) atomic basins;[39] the DI has sometimes been called the covalent bond order. It should be noted, however, that both gWBOs and DIs show a nearly linear correlation with the optimized bond lengths as exemplified by the data for S-N bonds for which $r^2 = 0.965$ irrespective of whether gWBOs or DIs are used in the analysis. Thus, the two sets of bond property values in Table 2 predict similar trends and underline the fact that, besides covalency, electrostatic interactions play a significant role in the short S-N and S-O distances in the investigated molecules and anions.[46,60,61,62] The importance of electrostatic interactions in bonding is mirrored in the shapes of MRCI-SD natural orbitals (see Fig. 2) as discussed above.

(Table 2 here)

(Table 3 here)

It is evident from Fig. 2 as well as from Table 2 that the replacement of O with S in SNO^- (to form SNS^-) has only a relatively minor effect on the electronic structure, leading to a change in the nature of the S-E bond towards more electrostatic interaction for E = S. The same is also true for the OSO/OSS and NSO^-/NSS pairs, in which case the S-E bond, however, transfers towards more covalent for E = S. The highest gWBOs and DIs are found for S-N bonds in NSS^- and NSO^-, of which the latter also shows the highest charge separation of all S-N bonds considered (3.71 e^-). Interestingly, recent theoretical calculations described a qualitatively similar bonding scheme for

the NSO^- anion but its S-O bond order was inferred to be only 0.75 with the help of Natural Resonance Theory (NRT) analysis.[17] In this respect, it is interesting that the authors did not include the Lewis structure with an S-N triple bond and an N-O single bond in the NRT analysis even though it is predicted to be the single best Lewis-type representation in Natural Bond Orbital (NBO) analysis. If this Lewis structure is explicitly included in NRT calculations, the predicted S-N and N-O bond orders of NSO^- become 2.40 and 1.40, respectively, in excellent agreement with the gWBOs reported herein. As a final note, it should be pointed out that the low gWBO calculated for OOO, 1.15 (see Table 2), is perfectly reasonable considering its diradical character and the occupation of the π-type antibonding orbital by almost 0.25 e^-.

Isomerization of SNS^- to NSS^-

Although the current calculations show NSS^- (**2b**) to be slightly more stable than SNS^- (**2a**), the symmetrical isomer has been proposed as the initial product of the electrochemical or chemical reduction of $SNSS^-$ (λ_{max} 465 nm) via cleavage of the S-S bond.[20,21] The formation of **2a** was inferred from the observation of new UV-visible absorption bands with λ_{max} 375 nm in acetonitrile or 390 nm in liquid NH_3, respectively. Our computed absorption maxima for SNS^- and NSS^- at MRCI-SD/def2-QZVP level of theory gave λ_{max} values of 342 and 327 nm, respectively; the corresponding PBE0/def2-QZVP values in acetonitrile are 353 and 333 nm. Since the computed absorption maxima of **2a** are closer to the experimental values than those of **2b**, these results support the formation of SNS^- via the process depicted in Scheme 1.

(Scheme 1 here)

The mechanism of isomerization of SNS^- (**2a**) to NSS^- (**2b**) was also explored computationally in order to establish the feasibility of the presence of **2a** in the reaction mixture. It has been reported for the related isomerization of NSO^- (**3a**) to SNO^- (**3b**$_2$) that the barrier for unimolecular transformation via the cyclic intermediate *c*-SNO^- is more than 450 kJ mol^{-1}.[16] Our PBE0/def2-QZVP calculations indicated that a similar unimolecular transformation between **2a** and **2b** is unfeasible and the conversion rather takes place via an asymmetric transition state with an activation barrier of 281 kJ mol^{-1} in acetonitrile. However, this barrier is still high enough that any **2a** formed in solution would not be converted to **2b** at room temperature.

An alternative route to isomerization of **2a** to **2b** is be the bimolecular reaction (eq. 1):

$$2\ SNS^- \rightleftharpoons SSN^- + SNS^- \qquad (1)$$

This pathway begins with an S-S bond formation that is immediately followed by an S-N interaction and a subsequent breakup of a second S-N bond to give the dianion $SNSNSS^{2-}$ (see Fig. 3). The proposed formation of this dianion finds support in the electrochemical one-electron reduction of cyclic 1,3-S_4N_2.[63] It was inferred to result in the formation of a radical monoanion, in which the extra electron enters the LUMO of 1,3-S_4N_2, an S-N antibonding orbital leading to dissociation.

(Fig. 3 here)

The final step on the predicted isomerization pathway involves the dissociation of the dianionic $SNSNSS^{2-}$ intermediate to SSN^- and SNS^-, hence, leading to partial rather than full isomerization. The highest activation energy on the pathway was found to be 107 kJ mol^{-1} in acetonitrile, which indicates that the conversion of different species should be relatively rapid at room temperature. Furthermore, the barrier is lowered to 82 kJ mol^{-1} with the inclusion of two explicit potassium cations that balance the negative charge (see Fig. 3). It is notable that the change in Gibbs energy upon dissociation of $SNSNSS^{2-}$ to SNS and NSS is calculated to be only 3 kJ mol^{-1} and, over time, the system should reach an equilibrium containing all three species in nearly equal amounts. As the calculated (PBE0/def2-QZVP) UV-visible absorption maxima of $SNSNSS^{2-}$ are 640, 439, 219, and 185 nm in acetonitrile, the formation of SNS^- upon reduction of $SNSS^-$ is not only plausible but also probable as it is the species with the best match between experimental and computed spectral parameters. Consequently, it should be possible to isolate salts of the binary sulphur-nitrogen anion S_2N^-, as either SNS^- (**2a**) or NSS^- (**2b**), with bulky organic cations or crown-ether solvated alkali-metal cations, similarly to what has been achieved for the isomeric anions NSO^- and SNO^-.[2,4,6,45] It might even be possible to isolate salts of the surprisingly stable dianion $SNSNSS^{2-}$.

Conclusions

The geometries, stabilities, and bonding of isomers of N_2S^{2-}, NSO^-, and NS_2^- have been explored at PBE0/def2-QZVP and MRCI-SD/def2-QZVP levels of theory; the neutral molecules SO_2, S_2O, S_3, and O_3 have been included for comparison. The energetically most favourable nitrogen-containing molecular species are the bent acyclic NSN^{2-} (**1a**), NSS^- (**2b**), and NSO^- (**3a**),

which all have the electropositive sulphur atom in the middle. However, the nitrogen-centered SNS^- (**2a**) and SNO^- (**3b**$_2$) isomers lie surprisingly close in energy to their more stable counterparts to allow for their occurrence. The experimental structural information for salts of NSN^{2-}, NSO^-, and SNO^- is in good agreement with the bond parameters yielded by the current calculations. The optimized geometries of OSO (**4a**), OSS (**5b**), and OOO (**7a**) also agree with the known metric parameters.

The bonding in all investigated species is qualitatively similar, though orbital and electron density analyses reveal important quantitative differences as well. The calculated generalized Wiberg bond orders reproduce well the formal bond orders expected on the basis of interatomic distances alone. A clear correlation between calculated delocalization indices and bond lengths is also seen, though the absolute values of delocalization indices are significantly less than formal bond orders, which highlights the importance of electrostatic interactions to bonding in the investigated species. For the majority of the most stable isomers, the ground state is dominated by a single configuration. The two notable and well-known exceptions are OOO (**7a**) and SSS (**6a**) that both have diradical character.

The proposed formation of SNS^- (**2a**) as the initial electrochemical or chemical reduction product of $SNSS^-$ is supported by the calculation of its UV-visible absorption maxima. While SNS^- lies only slightly higher in energy than the most stable isomer NSS^-, the barrier for their unimolecular interconversion is high. In contrast, the multi-step partial bimolecular isomerization process has a low activation barrier and is expected to proceed readily. The composition of the predicted equilibrium reaction mixture indicates that the solution should contain nearly equal amounts of SNS^-, SSN^-, and acyclic $SNSNSS^{2-}$, thereby rendering the detection of SNS^- via UV-visible spectroscopy probable. Finally, salts of the binary sulfur-nitrogen anion S_2N^- (as either **2a**

or **2b**) or $SNSNSS^{2-}$ with bulky organic cations or crown-ether solvated alkali-metal cations represent feasible synthetic targets, by comparison with the isolation and structural characterization of such salts for the related monoanions NSO^- and SNO^-.

Supplementary Material

Supplementary material (MRCI-SD/def2-QZVP energies and optimized atomic coordinates of all investigated species) is available with the article through the journal Web site at http://nrcresearchpress.com/doi/suppl/10.1139/cjc-2015-xxxx.

Acknowledgements

Financial support from the University of Jyväskylä (H.M.T and J.V.) and the Natural Sciences and Engineering Research Council of Canada (T.C.) is gratefully acknowledged. We are also grateful to the CSC – IT Center for Science Ltd for their generous provision of computational resources.

References

(1) For a review of the fundamental chemistry of binary S,N and ternary S,N,O anions, see Chivers, T.; Laitinen, R. S. *Chem. Soc. Rev*. **2017**, 46, 1357-1367. doi: 10.1039/C6CS00925E.

(2) Armitage, D. A.; Brand, J. C. *J.C.S., Chem. Comm*. **1979**, 1078-1079. doi: 10.1039/C39790001078.

(3) Herberhold, M.; Ehrenreich, W. *Angew. Chem., Int. Ed. Engl*. **1982**, *21*, 633-633. doi: 10.1002/anie.198206331.

(4) Heilemann, W.; Mews, R. *Chem. Ber*. **1988**, *121*, 461-463. doi: 10.1002/cber.19881210312

(5) Mann, S.; Jansen, M. *Z. Anorg. Chem. Allg. Chem.* **1995**, *621*, 153-158. doi: 10.1002/zaac.19956210128.

(6) Mann, S.; Jansen, M. *Z. Naturforsch*. **1994**, *49b*, 1503-1506. doi: 10.1515/znb-1994-1109

(7) Borrman, T.; Lork, E.; Mews, R.; Shakirov, M. M.; Zibarev, A. V. *Eur. J. Inorg. Chem.* **2004**, 2452-2458. doi: 10.1002/ejic.200300954.

(8) Lehman, J. H.; Lineberger, W. C. *J. Chem. Phys.* **2017**, *147*, 013943-1-013943-10. doi: 10.1063/1.4984129.

(9) For early examples, see Chivers, T. "*A Guide to Chalcogen-Nitrogen Chemistry",* World Scientific, Singapore, **2005**.

(10) Conti, M.; Trsic, M.; Laidlaw, W. G. *Inorg. Chem*. **1986**, *25*, 254-256. doi: 10.1021/ic00223a004.

(11) Bhattacharyya, A. A.; Bhattacharyya, A.; Adkins, R. R.; Turner, A. G., *J. Am. Chem. Soc.* **1981**, *103*, 7458-7465. doi: 10.1021/ja00415a010.

(12) Cortese-Krott, M. N.; Butler, A. R.; Woollins, J. D.; Feelisch, M. *Dalton Trans*. **2016**, *45*, 5908-5919, and references cited therein. doi: 10.1039/C5DT05034K.

(13) So, S. P. *Inorg. Chem.* **1989**, *28*, 2888-2890. doi: 10.1021/ic00313a036.

(14) Chivers, T.; Da Silva, A. B. F.; Treu, O. Jr.; Trsic, M. *J. Mol. Struct.* **1987**, *162*, 351-357. doi: 10.1016/0022-2860(87)87066-7.

(15) Ehrhardt, C.; Ahlrichs, R. *Chem . Phys.* **1986**, *108*, 417-428. doi: 10.1016/0301-0104(86)80109-4

(16) Trabelsi, T.; Yazidi, O.; Francisco, J. S.; Longuerri, R.; Hochlaf, M. *J. Chem. Phys*. **2015**, *143*, 164301-164310. doi: 10.1063/1.4933115.

(17) Labbow, R.; Michalik, D.; Reiss, F.; Schulz, A.; Villinger, A. *Angew. Chem., Int. Ed*. **2016**, *55*, 7680-7684. doi: 10.1002/anie.201601878.

(18) Miliordis, E.; Xantheas, S. S. *J. Am. Chem. Soc*. **2014**, *136*, 2808-2817, and references therein. doi: 10.1021/ja410726u.

(19) Lindquist, B. A.; Takeshita, T. Y.; Dunning, T. H. *J. Phys.Chem. A* **2016**, *120*, 2720-2726. doi: 10.1021/acs.jpca.6b02014.

(20) Chivers, T.; Hojo, M. *Inorg. Chem*. **1984**, *23*, 2738-2742. doi: 10.1021/ic00186a006.

(21) Dubois, P.; Lelieur, J. P.; Lepoutre, G. *Inorg. Chem*. **1989**, *28*, 2489-2491, and references cited therein. doi: 10.1021/ic00311a050.

(22) Bojes, J; Chivers, T.; Laidlaw, W. G.; Trsic, M. *J. Am. Chem. Soc*. **1982**, *104*, 4837-4841. doi: 10.1021/ja00382a017.

(23) Iraqi, M.; Goldberg, N.; Schwarz, H. *Chem. Ber*. **1994**, *127*, 1171-1173. doi: 10.1002/cber.19941270632.

(24) Trsic, M.; Laidlaw, W. G. *J. Mol. Struct*. **1985**, *123*, 259-265. doi: 10.1016/0166-1280(85)80169-X.

(25) Sannigrahi, A. B.; Peyerimhoff, S. D. *Chem. Phys. Lett.* **1990**, 175, 279-281. doi: 10.1016/0009-2614(90)80110-Y.

(26) Chen, J.-L.; Hu, W.-P. *J. Am. Chem. Soc.* **2011**, *133*, 16045-16053, and references cited therein. doi: 10.1021/ja203428x.

(27) *Gaussian 09, Revision D.01*, Frisch, M. J.; Trucks, G. W.; Schlegel, H. B.; Scuseria, G. E.; Robb, M. A.; Cheeseman, J. R.; Scalmani, G.; Barone, V.; Mennucci, B.; Petersson, G. A.; Nakatsuji, H.; Caricato, M.; Li, X.; Hratchian, H. P.; Izmaylov, A. F.; Bloino, J.; Zheng, G.; Sonnenberg, J. L.; Hada, M.; Ehara, M.; Toyota, K.; Fukuda, R.; Hasegawa, J.; Ishida, M.; Nakajima, T.; Honda, Y.; Kitao, O.; Nakai, H.; Vreven, T.; Montgomery, J. A., Jr.; Peralta, J. E.; Ogliaro, F.; Bearpark, M.; Heyd, J. J.; Brothers, E.; Kudin, K. N.; Staroverov, V. N.; Kobayashi, R.; Normand, J.; Raghavachari, K.; Rendell, A.; Burant, J. C.; Iyengar, S. S.; Tomasi, J.; Cossi, M.; Rega, N.; Millam, M. J.; Klene, M.; Knox, J. E.; Cross, J. B.; Bakken, V.; Adamo, C.; Jaramillo, J.; Gomperts, R.; Stratmann, R. E.; Yazyev, O.; Austin, A. J.; Cammi, R.; Pomelli, C.; Ochterski, J. W.; Martin, R. L.; Morokuma, K.; Zakrzewski, V. G.; Voth, G. A.; Salvador, P.; Dannenberg, J. J.; Dapprich, S.; Daniels, A. D.; Farkas, Ö.; Foresman, J. B.; Ortiz, J. V.; Cioslowski, J.; Fox, D. J. Gaussian, Inc., Wallingford CT, 2013.

(28) Perdew, J. P.; Burke, K.; Ernzerhof, M. *Phys. Rev. Lett*. **1996**, *77*, 3865-3868. doi: 10.1103/PhysRevLett.77.3865.

(29) Perdew, J. P.; Burke, K.; Ernzerhof, M. *Phys. Rev. Lett*. **1997**, *78*, 1396-1396. doi: 10.1103/PhysRevLett.78.1396.

(30) Perdew, J. P.; Ernzerhof, M.; Burke, K. *J. Chem. Phys*. **1996**, *105*, 9982-9985. doi: 10.1063/1.472933.

(31) Adamo, C.; Barone, V. *J. Chem. Phys*. **1999**, *110*, 6158-6170. doi: 10.1063/1.478522.

(32) Weigend, F.; Ahlrichs, R. *Phys. Chem. Chem. Phys.* **2005**, *7*, 3297-3305. doi: 10.1039/b508541a.

(33) Werner, H.-J.; Knowles, P. J.; Knizia, G.; Manby F. R.; Schütz, M. *WIREs Comput. Mol. Sci*. **2012**, *2*, 242-253. doi: 10.1002/wcms.82.

(34) *MOLPRO, version 2015.1*, a package of ab initio programs, Werner, H.-J.; Knowles, P. J.; Knizia, G.; Manby, F. R.; Schütz, M. and others. http://www.molpro.net/.

(35) Werner, H.-J.; Knowles, P. J. *J. Chem. Phys.* **1985**, *82*, 5053-5063. doi: 10.1063/1.448627.

(36) Knowles; P. J.; Werner, H.-J. *Chem. Phys. Lett.* **1985**, *115*, 259-267. doi: 10.1016/0009-2614(85)80025-7.

(37) Shamasundar, K.R.; Knizia, G.; Werner, H. J. *J. Chem. Phys.* **2011**, *135*, 054101-1-054101-17. doi: 10.1063/1.3609809.

(38) Mayer, I. *Chem. Phys. Lett.* **1983**, *97*, 270-274. doi: 10.1016/0009-2614(83)80005-0.

(39) Bader, R. F. W.; Stephens, M. E. *J. Am. Chem. Soc.* **1975**, *97*, 7391-7399. doi: 10.1021/ja00859a001.

(40) *Molden2AIM*, Zou, W. https://github.com/zorkzou/Molden2AIM/.

(41) *AIMAll*, *version 16.10.31*, Keith, T. A., TK Gristmill Software, Overland Park KS, USA, 2016. http://aim.tkgristmill.com/.

(42) *Jmol*: an open-source Java viewer for chemical structures in 3D. http://www.jmol.org/.

(43) For a recent review, see Tomasi, J.; Mennucci, B.; Cammi, R. *Chem. Rev.* **2005**, *105*, 2999-3093. doi: 10.1021/cr9904009.

(44) For a recent review, see Adamo, C.; Jacquemin, D. *Chem. Soc. Rev.* **2013**, *42*, 845-856. doi: 10.1039/c2cs35394f.

(45) Seel, F.; Kuhn, R.; Simon, G.; Wagner, M. *Z. Naturforsch.*, **1985**, *40b*, 1607-1617.

(46) Grabowsky, S.; Luger, P.; Buschmann, J.; Schneider, T.; Schirmeister, T.; Sobolev, A. N.; Jayatilaka, D. *Angew. Chem., Int. Ed.* **2012**, *51*, 6776-6779. doi: 10.1002/anie.201200745.

(47) Schenk, P. W.; Steudel, R. *Angew. Chem. Int. Ed. Engl.* **1964**, *3*, 61. doi: 10.1002/anie.196400611.

(48) Schenk, P. W.; Steudel, R. *Z. Anorg. Allg. Chem.* **1966**, *342*, 253-262. doi: 10.1002/zaac.19663420505.

(49) Marsden, C. J.; Smith, B. J. *Chem. Phys.* **1990**, *141*, 325-334. doi: 10.1016/0301-0104(90)87068-M.

(50) Tyuterev, Vl. G.; Tashkun, S.; Jensen, P.; Barbe, A.; Cours, T. *J. Mol. Spectrosc.* **1999**, *198*, 57-76. doi: 10.1006/jmsp.1999.7928.

(51) Millefiori, S.; Alparone, A. *J. Phys. Chem. A* **2001**, *105*, 9489-9497, and references cited therein. doi: 10.1021/jp0121466.

(52) Glezakov, V.-A.; Elbert, S. I.; Xantheas, S. S.; Ruedenberg, K. *J. Phys, Chem. A* **2010**, *114*, 8923-8931. doi: 10.1021/jp105025d.

(53) Miliordos, E.; Ruedenberg, K.; Xantheas, S. S. *Angew. Chem., Int. Ed.* **2013**, *52*, 5736-5739. doi: 10.1002/anie.201300654.

(54) Braida, B.; Galembeck, S. E.; Hiberty, P. C. *J. Chem. Theory Comput.* **2017**, *13*, 322, 3228-3235. doi: 10.1021/acs.jctc.7b00399.

(55) Miliordos, E.; Ruedenber, K.; Xantheas, S. S. *Angew. Chem. Int. Ed.* **2013**, *52*, 5736-5739. doi: 10.1002/anie.201300654.

(56) Bats, J. W.; Coppens, P.; Koetzle, T. F. *Acta Cryst., Sect. B* **1977**, *33*, 37-45. doi: 10.1107/S0567740877002568.

(57) Gregson, D.; Klebe, G.; Fuess, H. *Acta Cryst., Sect. C* **1991**, *47*, 1784-1786. doi: 10.1107/S0108270190011209.

(58) Groom, C. R.; Bruno, I. J.; Lightfoot, M. P; Ward, S. C. *Acta Cryst., Sect. B* **2016**, *72*, 171-179. doi: 10.1107/S2052520616003954.

(59) Santiso-Quinones, G.; Brueckner, R. Knapp, C.; Dionne, I.; Passmore, J.; Krossing, I. *Angew. Chem., Int. Ed.* **2009**, *48*, 1133-1137. doi: 10.1002/anie.200804021.

(60) Leusser, D.; Henn, J.; Kocher, N.; Engels, B.; Stalke, D. *J. Am. Chem. Soc.* **2004**, *126*, 1781-1793. doi: 10.1021/ja038941+.

(61) Henn, J.; Ilge, D.; Leusser, D.; Stalke, D.; Engels, B. *J. Phys. Chem. A* **2004**, *108*, 9442-9452. doi: 10.1021/jp047840a.

(62) Stalke, D. *Chem. Commun.* **2012**, *48*, 9559-9573. doi: 10.1039/c2cc33221c.

(63) Boeré, R. T.; Tuononen, H. M.; Chivers, T.; Roemmele, T. L., *J. Organomet. Chem.* **2007**, *692*, 2683-2696. doi:10.1016/j.jorganchem.2006.11.026.

Table 1. MRCI-SD/def2-QZVP optimized geometries and relative energies of the isomers of N_2S^{2-}, NS_2^-, NSO^-, SO_2, S_2O, S_3, and O_3.

Species	Isomer [a]	Parameter	MRCI-SD	Exptl.	Species	Isomer [a]	Parameter	MRCI-SD	Exptl.
N_2S^{2-}	NSN^{2-} (**1a**)	r_{NS} (Å)	1.532	1.484(3) [b]	**SO_2**	OSO (**4a**)	r_{OS} (Å)	1.431	1.4299(4) [c]
	C_{2v} ($^1A_1$)	α_{NSN} (°)	128.3	129.9(3) [b]		C_{2v} ($^1A_1$)	α_{OSO} (°)	119.5	117.16(3) [c]
		***E*$_{rel.}$ (kJ mol^{-1})**	**0**				***E*$_{rel.}$ (kJ mol^{-1})**	**0**	
	NNS^{2-} (**1b**)	r_{OO} (Å)	n.a. [d]			OOS (**4b**)	r_{OO} (Å)	1.301	
	C_s ($^1A'$)	r_{OS} (Å)	n.a. [d]			C_s ($^1A'$)	r_{OS}	1.632	
		α_{OOS} (°)	n.a. [d]				α_{OOS} (°)	119.5	
		***E*$_{rel.}$ (kJ mol^{-1})**	**n.a. [d]**				***E*$_{rel.}$ (kJ mol^{-1})**	**492**	
	c-NSN^{2-} (**1c**)	r_{NN} (Å)	1.501			*c*-OSO (**4c**)	r_{OS} (Å)	1.671	
	C_{2v} ($^1A_1$)	r_{NS} (Å)	1.793			C_{2v} ($^1A_1$)	r_{OO} (Å)	1.495	
		α_{NNS} (°)	65.2				α_{OSO} (°)	53.1	
		α_{NSN} (°)	49.5				α_{OOS} (°)	63.4	
		***E*$_{rel.}$ (kJ mol^{-1})**	**268**				***E*$_{rel.}$ (kJ mol^{-1})**	**466**	
NS_2^-	SNS^- (**2a**)	r_{NS} (Å)	1.649		**S_2O**	SOS (**5a**)	r_{OS} (Å)	1.633	
	C_{2v} ($^1A_1$)	α_{SNS} (°)	121.9			C_{2v} ($^1A_1$)	α_{SOS} (°)	124.3	
		***E*$_{rel.}$ (kJ mol^{-1})**	**25**				***E*$_{rel.}$ (kJ mol^{-1})**	**253**	
	NSS^- (**2b**)	r_{NS} (Å)	1.496			OSS (**5b**)	r_{OS} (Å)	1.468	1.456 [e]
	C_s ($^1A'$)	r_{SS} (Å)	2.036			C_s ($^1A'$)	r_{SS} (Å)	1.888	1.885 [e]
		α_{NSS} (°)	122.3				α_{OSS} (°)	118.0	117.9 [e]
		***E*$_{rel.}$ (kJ mol^{-1})**	**0**				***E*$_{rel.}$ (kJ mol^{-1})**	**0**	
	c-SNS^- (**2c**)	r_{NS} (Å)	1.780			*c*-SOS (**5c**)	r_{OS} (Å)	1.715	
	C_{2v} ($^1A_1$)	r_{SS} (Å)	2.043			C_{2v} ($^1A_1$)	r_{SS} (Å)	2.038	
		α_{NSS} (°)	55.0				α_{SOS} (°)	72.9	
		α_{SNS} (°)	70.0				α_{OSS} (°)	53.5	
		***E*$_{rel.}$ (kJ mol^{-1})**	**177**				***E*$_{rel.}$ (kJ mol^{-1})**	**186**	

NSO⁻	NSO⁻ (**3a**)	r_{NS} (Å)	1.477	1.431(8) [f]	**S_3**	SSS (**6a**)	r_{SS} (Å)	1.925	
	C_s ($^1A'$)	r_{OS}	1.501	1.438(7) [f]		C_{2v} ($^1A_1$)	α_{SSS} (°)	117.7	
		α_{NSO} (°)	124.0	126.8(4) [f]			**$E_{rel.}$ (kJ mol^{-1})**	**0**	
		$E_{rel.}$ (kJ mol^{-1})	**0**			*c*-SSS (**6c**)	r_{SS} (Å)	2.085	
	SNO⁻ (**3b$_1$**)	r_{NO} (Å)	1.236	1.214(5) [g]		D_{3h} ($^1A_1$)	α_{SSS} (°)	60.0	
	C_s ($^1A'$)	r_{NS}	1.727	1.695(4) [g]			**$E_{rel.}$ (kJ mol^{-1})**	**28**	
		α_{ONS} (°)	117.8	120.5(3) [g]					
		$E_{rel.}$ (kJ mol^{-1})	**89**		**O_3**	OOO (**7a**)	r_{OO} (Å)	1.272	1.27276(15) [h]
	NOS⁻ (**3b$_2$**)	r_{ON} (Å)	1.285			C_{2v} ($^1A_1$)	α_{OOO} (°)	116.8	116.754(3) [h]
	C_s ($^3A''$)	r_{OS}	1.821				**$E_{rel.}$ (kJ mol^{-1})**	**0**	
		α_{NOS} (°)	115.0			*c*-OOO(**7c**)	r_{OO} (Å)	1.439	
		$E_{rel.}$ (kJ mol^{-1})	**308**			D_{3h} ($^1A_1$)	α_{OOO} (°)	60.0	
	c-NSO⁻ (**3c**)	r_{NO} (Å)	1.546				**$E_{rel.}$ (kJ mol^{-1})**	**132**	
	C_s ($^1A'$)	r_{NS} (Å)	1.741						
		r_{OS} (Å)	1.674						
		α_{ONS} (°)	60.9						
		α_{SON} (°)	65.3						
		α_{NSO} (°)	53.8						
		$E_{rel.}$ (kJ mol^{-1})	**364**						

[a] Chemical formula, numerical abbreviation, point group, and ground state term. [b] Ref. 7. [c] Ref. 46. [d] Not a stable species in vacuum. [e] Ref. 49. [f] Ref. 7. [g] Ref. 45. [h] Ref. 50.

Table 2. Bond lengths, generalized Wiberg bond orders, AIM delocalization indices, and AIM atomic charges of **1a**, **2a**, **2b**, **3a**, **3b**$_1$, **4a**, **5b**, **6a**, and **7a**.[a]

Species	Bond	Bond length (Å)	Generalized Wiberg bond order	AIM delocalization index	AIM atomic charges	
NSN^{2-} (**1a**)	S-N	1.532	1.88	1.42	N:	−1.83
					S:	1.67
					N:	−1.83
SNS^- (**2a**)	S-N	1.649	1.22	1.27	S:	0.11
					N:	−1.23
					S:	0.11
NSS^- (**2b**)	S-N	1.496	2.06	1.57	N:	−1.41
					S:[b]	1.14
	S-S	2.036	1.21	1.21	S:[c]	−0.73
NSO^- (**3a**)	S-N	1.477	2.21	1.53	N:	−1.64
					S:	2.05
	S-O	1.501	1.40	1.08	O:	−1.41
SNO^- (**3b**$_1$)	S-N	1.727	1.11	1.14	S:	−0.31
					N:	−0.13
	N-O	1.236	1.39	1.43	O:	−0.56
OSO **(4a)**	S-O	1.431	1.84	1.16	O:	−1.28
					S:	2.55
					O:	−1.28
OSS (**5b**)	S-O	1.468	1.69	1.22	O:	−1.19
					S:[b]	1.33
	S-S	1.888	1.75	1.57	S:[c]	−0.14
SSS (**6a**)	S-S	1.925	1.49	1.40	S:[c]	−0.10
					S:[b]	0.19
					S:[c]	−0.10
OOO (**7a**)	O-O	1.272	1.15	1.17	O:[c]	−0.10
					O:[b]	0.20
					O:[c]	−0.10

[a] MRCI-SD/def2-QZVP level. [b] Central atom. [c] Terminal atom.

Table 3. Typical S-N, S-O and S-S single and double bond lengths (Å)

Bond	Single bond	Example	Double bond	Example
S-N	1.7714(4)	H_3NSO_3 [a]	1.544(2)	$(NSF)_4$ [b]
S-O	1.644(17)	R_1SOR_2 [c]	1.492(1)	R_1R_2SO[c]
S-S	2.0529(2)	S_8 [d]	1.908(16)	$(RO)_2SS$[c]

[a] Ref. 56. [b] Ref. 57. [c] Mean value of several related species from the Cambridge Crystallographic Data Base (Ref. 58) [d] Ref. 59.

Fig. 1. Common Lewis-type representations of the isomers of N_2S^{2-}, NS^{2-}, NSO^{-}, SO_2, S_2O, S_3, and O_3 (formal charges indicated with coloured numbers).

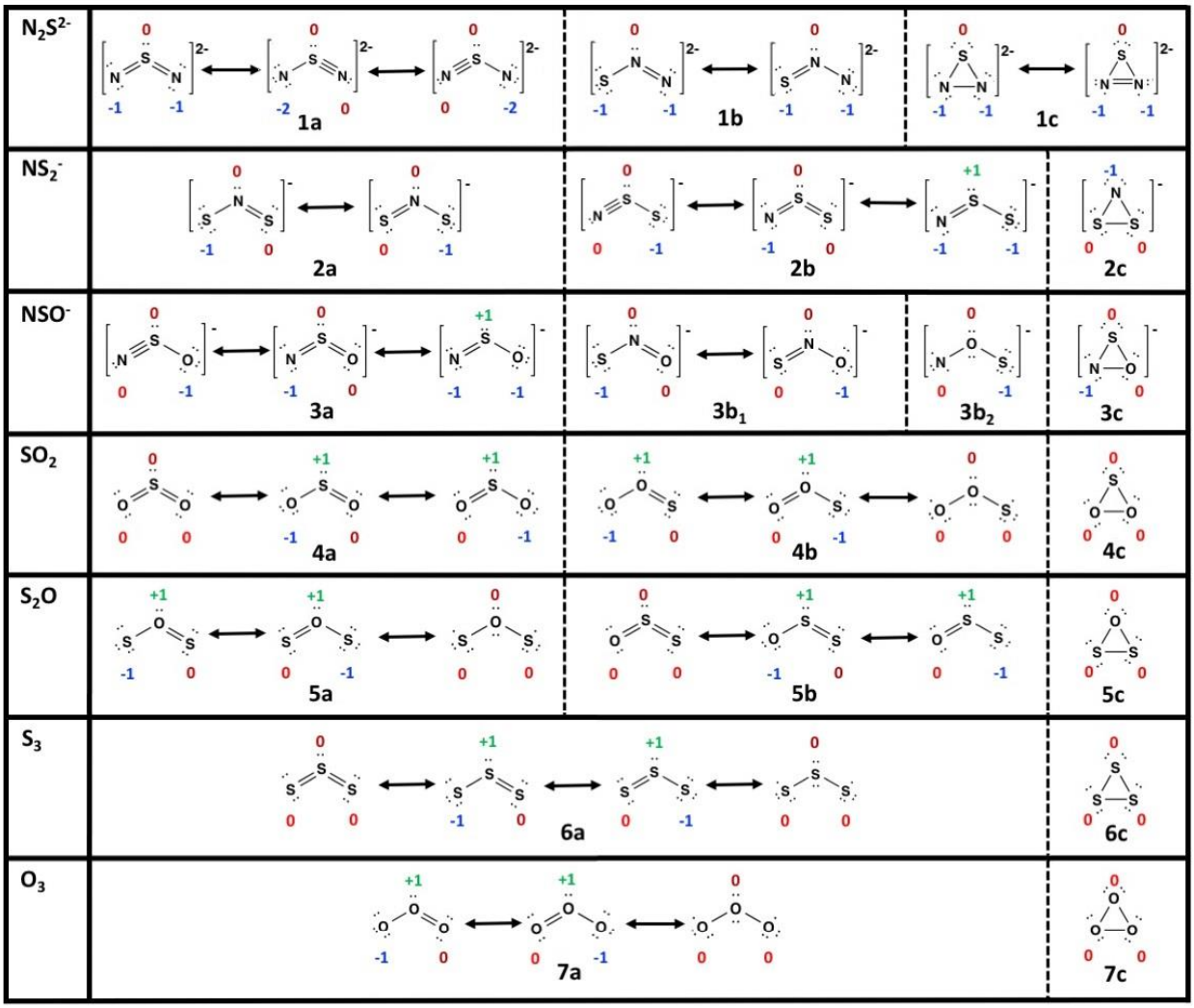

Fig. 2. The occupancies of formally occupied (blue) and unoccupied (green) MRCI-SD natural orbitals of NSN^{2-} (**1a**), SNS^{-} (**2a**), NSS^{-} (**2b**), NSO^{-} (**3a**), SNO^{-} (**3b$_1$**), and OSO (**4a**).

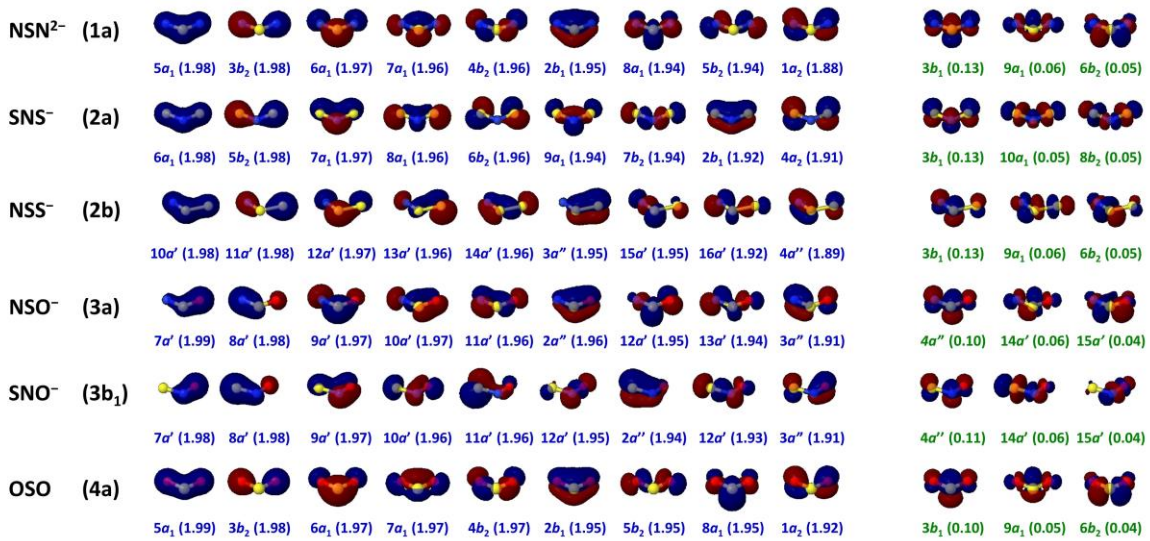

Fig. 3. Calculated reaction pathway for the partial bimolecular isomerization of SNS^- (**2a**) to NSS^- (**2b**) (colour code: S = yellow, N = light blue, and K = grey).

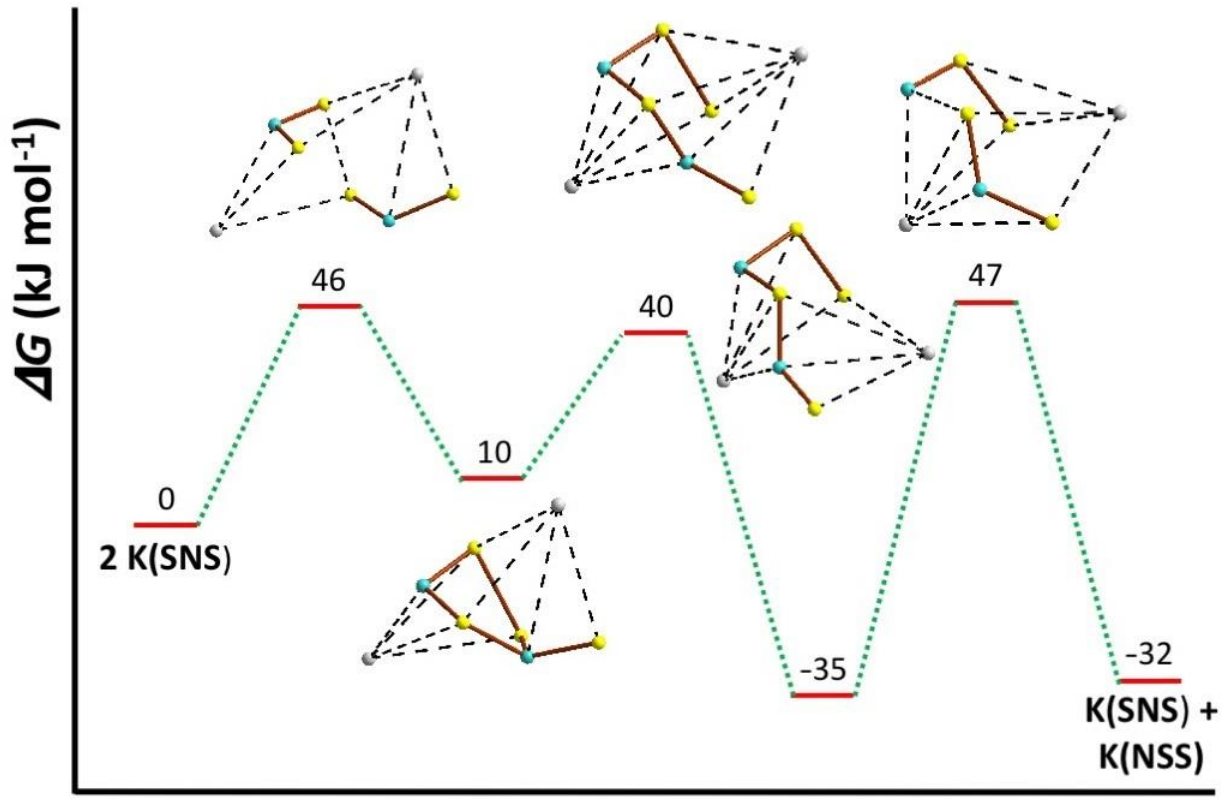

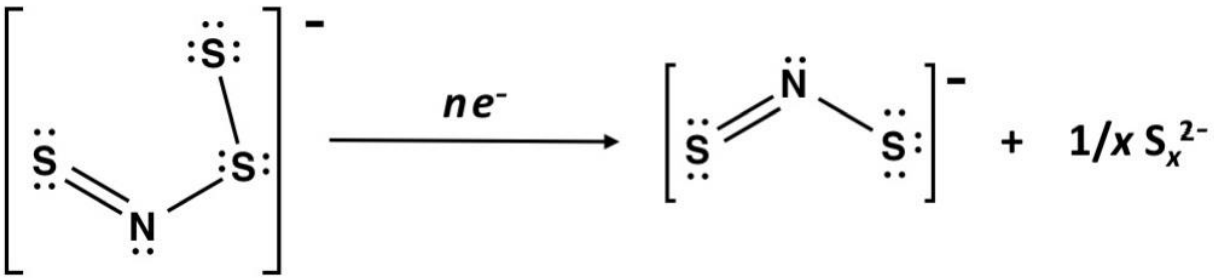

Scheme 1. Proposed formation of SNS^- (**2a**) via electrochemical reduction of $SNSS^-$.

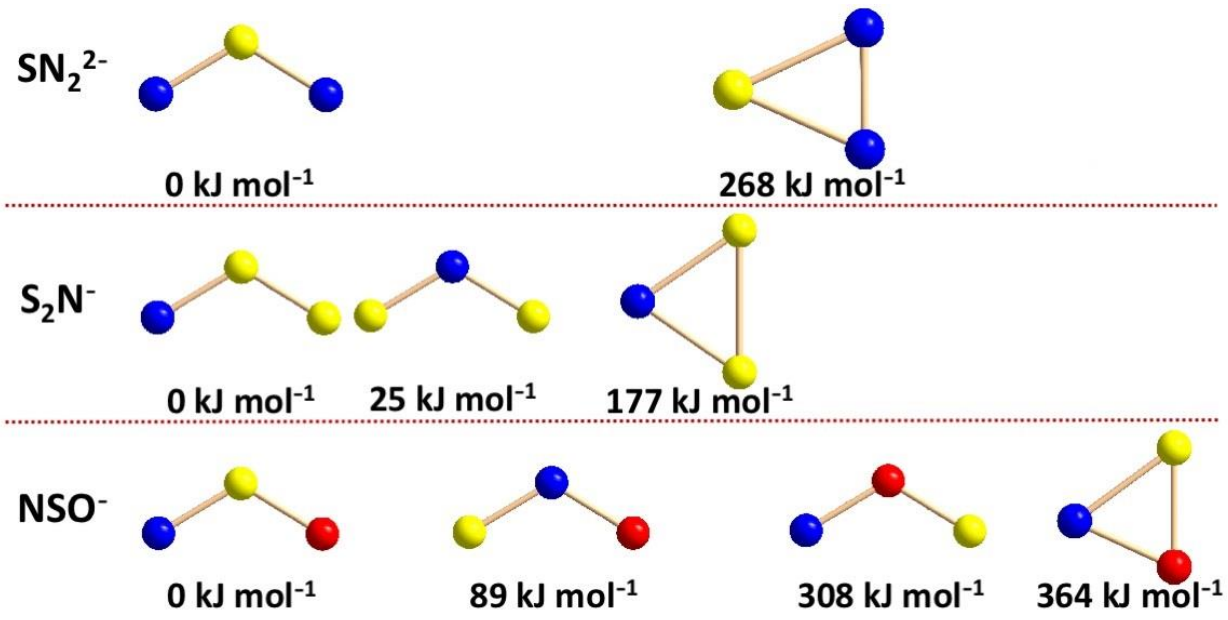

Graphical abstract